

Comparing convolution-integral models with analytical pipe-flow solutions

K Urbanowicz¹, A S Tijsseling² and M Firkowski¹

¹ West Pomeranian University of Technology Szczecin, Faculty of Mechanical Engineering and Mechatronics, Al Piastów 19, 70-310 Szczecin, Poland

² Eindhoven University of Technology, Department of Mathematics and Computer Science, PO Box 513, 5600 MB Eindhoven, The Netherlands

Abstract. This paper presents and discusses known analytical solutions for accelerated laminar pipe flow. On the basis of these solutions, formulas are given that enable the determination of shear stresses on the pipe walls together with a formula for coefficients of non-stationary friction losses. A small extension is introduced, which will make it possible to analyse flow in pipes inclined at any angle. Besides solutions related to acceleration, this paper also examines the analytical solution for decelerated laminar flow and the solution for flow changing its direction in both a stepwise and a linear manner. Calculations based on the analytical formulas are compared with numerical results obtained by Zielke's convolution-integral method. The convolution integral is treated both in the classical way and in a novel more efficient way. The classical approach requires the knowledge of the complete history of the flow, which makes it computationally inefficient and memory-wise burdensome. In the efficient calculation, only the velocity changes taking place in the last three time steps are needed.

1. Introduction

Over the last 150 years, many papers have been written on the flow of liquids in water supply systems, oil pipelines, blood vessels, and heating and cooling systems. Most of them concerned the analysis of steady states. A minority of authors dealt with transient states occurring in pipes during the first seconds after disturbing the established steady flow. The analytical solutions obtained in [1-4] required extensive knowledge of mathematics. These papers were written a long time ago, not always easy to obtain and not in English. Therefore they were largely forgotten by the scientific community. Only the progressing digitisation of many libraries, their free use through the global internet, and tools like Google Translate and Play, have made them accessible.

This year, 145 years have passed since the first publication of the analytical solution for the accelerated flow of an incompressible viscous fluid in a hydraulic pipeline or mammal blood vessel. The solution was presented in 1871 by Roiti at the University of Pisa in the university's first volume of their scientific journal [1]. Roiti developed a solution for unsteady flow in vertical pipes that was mainly based on earlier work in the field of unsteady heat transfer in cylinders by Poisson [5-7] and Betti [8,9]. Due to the local nature of the publication and the absence of English, French or German translations, this solution remained unknown for a long time after its publication. Even the Italian Fassò [10] did not refer to it sixty years ago and we think that it is still unknown to today's scientific community. Eleven years later, in 1882, Gromeka at the University of Kazan developed a similar solution but for horizontal pipes [2]. This solution stayed obscure for the same reasons as pointed out above, but finally became known to the scientific community [11].



Many years later, a similar problem was focused upon and studied by Szymański. While in 1928 staying in Paris on an internship, Szymański derived his solution which was based mainly on Fourier-Bessel series. The final works [3,12] contained a range of mathematical proofs on convergence and asymptotic behaviour of the analytical solutions. Yet another approach to find exactly the same solution was published in 1951 by Gerbes [4], who used the Laplace transform. Gerbes, besides showing the solution to accelerated flow, also proposed a solution for decelerated flow (the complete and rapid disappearance of the pressure gradient along the pipe was considered). The current study will also deal with other known analytical solutions, such as those presented in 1978 by Chambré et al [13], who analyzed flow reversal as a result of both a step change and a ramp change of the pressure gradient.

The main objective of this study is the comparison of the classic analytical solutions with solutions obtained by applying efficient numerical methods to the corresponding convolution integrals. Integral convolution models are widely used to introduce unsteady friction in numerical methods based on a mesh with fixed time steps (especially the method of characteristics). The results of the numerical simulations show that the conventional numerical solution [14] and a much more effective solution [15] are entirely consistent with the classic analytical results.

2. Analytical solutions for accelerating laminar flow

The oldest of the papers described below has been found quite by chance, while collecting materials on Gromeka. Attempts to find the papers of the Italian academic Betti, who, among other things, dealt with studies of transient heat flows [8,9], resulted in finding the forgotten work by Roiti, which will be discussed briefly below. Roiti worked at the same university (University of Pisa) as Betti, so he had a direct opportunity to study the work of his older colleague, which was especially important in an era where transfer of information, even written down, was limited.

2.1. Vertical accelerating pipe flow

The Roiti paper discussed below, entitled "Sul movimento dei liquidi" ("On the movement of liquid"), relates to transient flow in pipes and is probably the first work on this subject. Roiti, in order to find his solution, used the method for calculating transient heat flow in cylinders that was described three years earlier by Betti [8,9]. Roiti analysed accelerated flow of liquids in a vertical pipe. The hydrodynamic equation describing this type of incompressible flow reads:

$$g - \frac{1}{\rho} \frac{\partial p}{\partial x} = \frac{\partial v}{\partial t} - v \left(\frac{\partial^2 v}{\partial r^2} + \frac{1}{r} \frac{\partial v}{\partial r} \right) = \frac{\partial v}{\partial t} - \frac{v}{r} \frac{\partial}{\partial r} \left(r \frac{\partial v}{\partial r} \right), \quad (1)$$

where: r - radial coordinate [m], x - axial coordinate [m], t - time [s], v - flow velocity [m/s], p - pressure [Pa], g - acceleration due to gravity [m/s²], ν - kinematic viscosity [m²/s].

The solution of Eq. (1), for a suddenly applied pressure gradient and gravity acting vertically, was presented in the last chapter of Roiti's work in the form:

$$v(r, t)_{\text{ver.}} = \frac{2}{\nu R} \left(g + \frac{\Delta p}{\rho L} \right) \sum_{n=1}^{\infty} \frac{J_0(\lambda_n r)}{\lambda_n^3 J_1(\lambda_n R)} \left(1 - e^{-\lambda_n^2 \hat{t}} \right) = \frac{2R^2}{\nu} \left(g + \frac{\Delta p}{\rho L} \right) \sum_{n=1}^{\infty} \frac{J_0\left(\lambda_n \frac{r}{R}\right)}{\lambda_n^3 J_1(\lambda_n)} \left(1 - e^{-\lambda_n^2 \hat{t}} \right), \quad (2)$$

where: $\lambda_n = \chi_n/R$ - the n^{th} zero of the Bessel function of type J_0 , $\hat{t} = \nu t/R^2$ - dimensionless time.

It is an expanded solution for the velocity profile in the horizontal cross-section of the vertical pipe. Roiti, with use of above formula, also determined a formula for the cross-sectional average value of the flow velocity, which is particularly useful in one-dimensional models:

$$v_{\text{m, ver.}} = \frac{2}{R^2} \int_0^R r \cdot v(r, \hat{t}) dr = \frac{4R^2}{\nu} \left(g + \frac{\Delta p}{\rho L} \right) \sum_{n=1}^{\infty} \frac{1 - e^{-\lambda_n^2 \hat{t}}}{\lambda_n^4} = \left(\frac{R^2}{8\mu L} (g\rho L + \Delta p) \right) \left(1 - 32 \sum_{n=1}^{\infty} \frac{e^{-\lambda_n^2 \hat{t}}}{\lambda_n^4} \right). \quad (3)$$

Besides the theoretical part, Roiti's paper is distinguished by reporting a series of experimental tests carried out in a local laboratory which purpose was to confirm his newly derived formulas. But Roiti was not fully satisfied with the results, because he did not achieve full compliance of theory and experiment. The analytical results were characterised by a very good compatibility at low velocities, but significant deviations of measured results from theory was observed for higher velocities. It is difficult to clearly assess now, but perhaps these deviations were caused by the change in the nature of flow from laminar (for which the formulas were derived) to turbulent. At the time of publication of his paper, the volatile nature of turbulent flow had not been discovered yet; only twelve years later Reynolds published his most famous work [16].

For the purpose of conducting numerical studies in this paper, formulas for the shear stress on the pipe wall (4) and the temporary coefficient of resistance (5) for this type of flow have been determined:

$$\tau_{w,ver.} = \frac{R}{2} \left(\gamma + \frac{\Delta p}{L} \right) \left[1 - 4 \sum_{n=1}^{\infty} \frac{e^{-\lambda_n^2 \hat{t}}}{\lambda_n^2} \right] = \frac{4\mu}{R} v_{\infty,ver.} \left[1 - 4 \sum_{n=1}^{\infty} \frac{e^{-\lambda_n^2 \hat{t}}}{\lambda_n^2} \right], \quad (4)$$

$$f_{ver.} = \frac{8\tau_{w,ver.}}{\rho \cdot v_{m,ver.}^2} = \frac{64}{Re_{\infty,ver.}} \left[1 - 4 \sum_{n=1}^{\infty} \frac{e^{-\lambda_n^2 \hat{t}}}{\lambda_n^2} \right] \cdot \left[1 - 32 \sum_{n=1}^{\infty} \frac{e^{-\lambda_n^2 \hat{t}}}{\lambda_n^4} \right]^{-2}, \quad (5)$$

where: $\gamma = \rho g$ - specific weight of the liquid; $Re = (v_{\infty,ver.} \cdot D)/\nu$ and:

$$v_{\infty,ver.} = \left(\frac{R^2}{8\mu L} (g\rho L + \Delta p) \right). \quad (6)$$

2.2. Horizontal accelerating pipe flow

The Szymański paper [3] is widely known and repeatedly cited [17-26] and deals with accelerated flow in horizontal pipes. It contains a range of mathematical proofs on convergence and asymptotic behaviour of the derived solutions. In the 1930s that was most useful, since there were no computers to carry out quick calculational checks. More about Szymański's work and life can be read in the authors' recent paper [27]. However, it has been pointed out more and more often that an identical solution was also found by Gromeka [11,28,29]. He wrote in Russian and his paper was published in research communications of the university of Kazan [2]. This paper, however, still remains inaccessible to the wider public. Fortunately, a book published on the occasion of the hundred-year anniversary of Gromeka's birth contains his collected works [30]. It can be accessed via the internet [31]; the only problem might be the language barrier, since none of Gromeka's papers has been translated into English, French or German.

Both Gromeka and Szymański have sought a solution for the partial differential equation (1) assuming the absence of body forces ($g=0$). They independently presented an analogous final solution for the time-dependent velocity profile in the form:

$$v(r, \hat{t})_{hor.} = 2v_{\infty,hor.} \left[\left[1 - \left(\frac{r}{R} \right)^2 \right] - 8 \sum_{n=1}^{\infty} \frac{J_0 \left(\lambda_n \cdot \frac{r}{R} \right)}{\lambda_n^3 \cdot J_1(\lambda_n)} \cdot e^{-\lambda_n^2 \hat{t}} \right], \text{ where: } v_{\infty,hor.} = \frac{R^2 \Delta p}{8\mu L}. \quad (7)$$

From the above formula, as previously from Eq. (3), we can determine the formula for the average velocity:

$$v_{m,hor.} = v_{\infty,hor.} \left[1 - 32 \sum_{n=1}^{\infty} \frac{e^{-\lambda_n^2 \hat{t}}}{\lambda_n^4} \right], \quad (8)$$

and the shear stress:

$$\tau_{w,hor.} = \frac{4\mu}{R} v_{\infty,hor.} \left[1 - 4 \sum_{n=1}^{\infty} \frac{e^{-\lambda_n^2 \hat{t}}}{\lambda_n^2} \right] = \frac{R\Delta p}{2L} \left[1 - 4 \sum_{n=1}^{\infty} \frac{e^{-\lambda_n^2 \hat{t}}}{\lambda_n^2} \right]. \quad (9)$$

Just as in the previous section, the instantaneous coefficient of resistance has been designated:

$$f_{hor.} = \frac{8\tau_{w,hor.}}{\rho \cdot v_{m,hor.}^2} = \frac{64}{Re_{\infty,hor.}} \left[1 - 4 \sum_{n=1}^{\infty} \frac{e^{-\lambda_n^2 \hat{t}}}{\lambda_n^2} \right] \cdot \left[1 - 32 \sum_{n=1}^{\infty} \frac{e^{-\lambda_n^2 \hat{t}}}{\lambda_n^4} \right]^{-2}. \quad (10)$$

The latter will be useful in the calculations presented in Section 3.

2.3. General solution

Analysis of the above formulas, known from the literature, shows no immediate relation between the flow in horizontal (Gromeka, Szymański) and vertical (Roiti) pipes. In practice, hydraulic lines are often installed at different angles and are used in devices with variable use (for example excavators), in which the slope of the pipe depends on the actual situation. With this in mind, we suggest a universal form of the above formulas, in terms of piezometric heads as in steady flow [32]:

$$v(r, t) = \frac{2R^2}{v} \left(\frac{\Delta p}{\rho L} - g \sin \alpha \right) \sum_{n=1}^{\infty} \frac{J_0 \left(\lambda_n \frac{r}{R} \right)}{\lambda_n^3 J_1(\lambda_n)} \left(1 - e^{-\lambda_n^2 \hat{t}} \right), \quad (11)$$

$$v_m = \left(\frac{R^2}{8\mu L} (\Delta p - g\rho L \sin \alpha) \right) \left(1 - 32 \sum_{n=1}^{\infty} \frac{e^{-\lambda_n^2 \hat{t}}}{\lambda_n^4} \right), \quad (12)$$

$$\tau_w = \frac{4\mu}{R} v_{\infty} \left[1 - 4 \sum_{n=1}^{\infty} \frac{e^{-\lambda_n^2 \hat{t}}}{\lambda_n^2} \right] \quad \text{where} \quad v_{\infty} = \left(\frac{R^2}{8\mu L} (\Delta p - g\rho L \sin \alpha) \right). \quad (13)$$

$$f = \frac{8\tau_w}{\rho \cdot v_m^2} = \frac{64}{Re_{\infty}} \left[1 - 4 \sum_{n=1}^{\infty} \frac{e^{-\lambda_n^2 \hat{t}}}{\lambda_n^2} \right] \cdot \left[1 - 32 \sum_{n=1}^{\infty} \frac{e^{-\lambda_n^2 \hat{t}}}{\lambda_n^4} \right]^{-2}. \quad (14)$$

From the above equations, it can be seen that the flow in a horizontal pipe (Gromeka-Szymański solution) is at an angle $\alpha = 0^\circ$ (Eqs. 7-10). For angles in the range $0^\circ < \alpha < 90^\circ$, upward flow occurs if the pressure gradient overcomes gravity, while for angles in the range $-90^\circ < \alpha < 0^\circ$, there is a downward flow (Fig. 1), up to the extreme case of $\alpha = -90^\circ$ for which the above formulas are reduced to the form derived by Roiti (Eqs. 2-5).

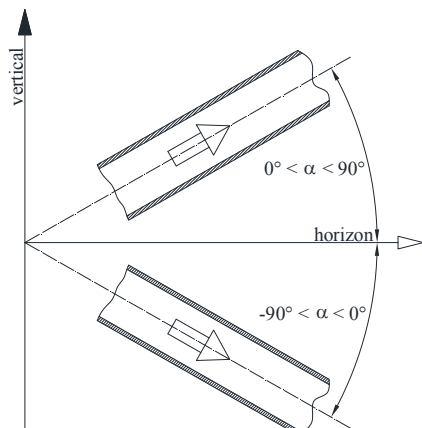


Figure 1. The tilt angle of the pipe and the positive direction of fluid flow.

To facilitate calculations, infinite sums appearing in the above formulas are saved in the selected range in the form of finite sums of exponential expressions. Thus, there is no need for the numerical determination of zeros of the Bessel function. For a single calculation of the coefficients, we can use the improved calculation algorithm presented in the first author's paper [33]. The improvement consists in the fact that both the current values of coefficients m_i and n_i can be calculated from precise mathematical formulas, such as:

$$\frac{C1 - C2}{\exp(-n_{i+1} \cdot E1)} - \frac{C3 - C4}{\exp(-n_{i+1} \cdot E2)} = 0, \quad (15)$$

where: C1, ..., C4 and E1 and E2 are constants changing during the calculation of subsequent coefficients, which can be calculated analytically from

$$\ln\left(\frac{C2 - C1}{C4 - C3}\right) \cdot (E2 - E1)^{-1} = n_{i+1}, \quad (16)$$

and not numerically as was mentioned in that particular paper (the author apologizes for this oversight). The resulting exponential functions presented below, which we will call weighting functions, will guarantee a high compatibility with the original infinite sums in the practical use of them, i.e. for \hat{t} from 10^{-10} to ∞ . The three new functions have the form:

$$\left(1 - 32 \sum_{n=1}^{\infty} \frac{e^{-\lambda_n^2 \hat{t}}}{\lambda_n^4}\right) = w_{\text{vsr}}^{-1}(\hat{t}) = \left[\sum_{i=1}^{22} a_i e^{-b_i \hat{t}}\right]^{-1}, \quad (17.1)$$

$$\left[1 - 4 \sum_{n=1}^{\infty} \frac{e^{-\lambda_n^2 \hat{t}}}{\lambda_n^2}\right] = w_{\text{r}}^{-1}(\hat{t}) = \left[\sum_{i=1}^{22} c_i e^{-d_i \hat{t}}\right]^{-1}, \quad (17.2)$$

$$\left[1 - 4 \sum_{n=1}^{\infty} \frac{e^{-\lambda_n^2 \hat{t}}}{\lambda_n^2}\right] \cdot \left[1 - 32 \sum_{n=1}^{\infty} \frac{e^{-\lambda_n^2 \hat{t}}}{\lambda_n^4}\right]^{-2} = w_{\text{fc}}(\hat{t}) = \sum_{i=1}^{22} e_i e^{-f_i \hat{t}}. \quad (17.3)$$

The values of the coefficients a_i , b_i , c_i , d_i , e_i and f_i obtained from the necessary calculations are summarised in Table 1 below.

Table 1. Calculated coefficients of the weighting functions.

i	a_i	b_i	c_i	d_i	e_i	f_i
1	1	0	1	0	1	0
2	1.1253	6.0053	0.7768	5.9421	1.5934	6.1776
3	2.7127	16.9400	1.0324	16.0510	6.0640	18.9757
4	8.0364	51.0539	1.9851	49.0212	27.9438	59.4110
5	24.3347	159.321	3.5383	153.327	140.1346	188.4939
6	74.931	502.258	6.3077	482.664	738.0994	598.58
7	233.297	1587.478	11.228	1524.031	4000.341	1898.58
8	731.22	5020.45	19.972	4817.25	22034.287	6015.23
9	2300.67	15878.53	35.520	15231.6	122474.44	19043.41
10	7254.65	50218	63.167	48165.3	684236.73	60260.3
11	22904.4	158817	112.33	152311	3833635.8	190631.9
12	72365	502249	199.75	481651	21513643	602960.7
13	228721	1588296	355.22	1523114	120839597	1906961
14	723072	5022718	631.67	4816511	679086243	6030748
15	2286156	15883308	1123.29	15231148	3817303983	19071499
16	7228764	50227233	1997.53	48165125	21462087350	60310528
17	22858248	158832515	3552.16	152311507	120668249757	190717542
18	72279258	502266929	6316.75	481651411	678652175201	603131809
19	228234286	1587473790	11232.9	1523116816	3812553675009	1906802180
20	721051335	5014638487	19975.3	4816508100	21394602492353	6024041424
21	2274403251	15835931280	35521.4	15231092712	120019731059804	19023982623
22	7327599236	50349124336	63165.7	48164347598	674994401528792	60136925028

2.4. Horizontal decelerating pipe flow

Gerbes in his 1951 paper [4] used the Laplace transform. Starting from the Navier-Stokes equations for incompressible viscous liquid, he obtained the same formula (7) for the velocity profile in accelerated laminar flow as Gromeka and Szymański. In addition, Gerbes was the only one interested in the deceleration of the fluid. He presented the final formula for the velocity profile in a cross-section of the pipe during stopping in the following form:

$$v(r, \hat{t}) = \frac{R^2 \Delta p}{4\mu L} \sum_{n=1}^{\infty} \frac{8J_0(\lambda_n \frac{r}{R})}{\lambda_n^3 J_1(\lambda_n)} \cdot e^{-\lambda_n^2 \hat{t}}. \quad (18)$$

By taking the average velocity of steady flow before the start of the deceleration as:

$$v_0 = \frac{R^2 \Delta p}{8\mu L}, \quad (19)$$

we obtain

$$v(r, \hat{t})_d = v_0 \sum_{n=1}^{\infty} \frac{16J_0(\lambda_n \frac{r}{R})}{\lambda_n^3 J_1(\lambda_n)} \cdot e^{-\lambda_n^2 \hat{t}}. \quad (20)$$

Calculating the average velocity for decelerated flow gives:

$$v_{m,d} = \frac{2}{R^2} \int_0^R r \cdot v(r, \hat{t}) dr = v_0 \sum_{n=1}^{\infty} \frac{32}{\lambda_n^4} \cdot e^{-\lambda_n^2 \hat{t}} = \frac{4R^2 \Delta p}{\mu L} \sum_{n=1}^{\infty} \frac{e^{-\lambda_n^2 \hat{t}}}{\lambda_n^4}. \quad (21)$$

In contrast to acceleration, the shear stress on the pipe wall ($r=R$) during deceleration is:

$$\tau_{w,d} = -\mu \frac{\partial v(r, \hat{t})}{\partial r} = \frac{v_0 \cdot \mu}{R} \sum_{n=1}^{\infty} \frac{16}{\lambda_n^2} \cdot e^{-\lambda_n^2 \hat{t}} = \frac{2R \Delta p}{L} \sum_{n=1}^{\infty} \frac{e^{-\lambda_n^2 \hat{t}}}{\lambda_n^2}. \quad (22)$$

The coefficient of resistance in decelerated flow, on the basis of the above formulas, is calculated herein with the formula:

$$f_d = \frac{64}{Re_0} \left[4 \sum_{n=1}^{\infty} \frac{e^{-\lambda_n^2 \hat{t}}}{\lambda_n^2} \right] \cdot \left[32 \sum_{n=1}^{\infty} \frac{e^{-\lambda_n^2 \hat{t}}}{\lambda_n^4} \right]^{-2} \quad \text{where} \quad Re_0 = \frac{D \cdot v_0}{\nu}. \quad (23)$$

2.5. Reversed flow solution

Still another solution, which uses the finite Hankel transform, was derived in 1978 by a group of researchers under the leadership of Chambré [13]. It concerns reverse flow, which occurs after a sudden (stepwise) or a linear (ramp) change of the sign of the pressure gradient forcing the movement of the liquid. It is a kind of combination of accelerated flow with decelerated flow. This type of flow occurs, for example, in the cases of loss of coolant accidents in water reactors. In the case of an immediate change of the sign of the pressure gradient, the derived solutions were as follows:

$$v(r, t)_r = v_{\infty} \sum_{n=1}^{\infty} \frac{16 \cdot J_0\left(\lambda_n \frac{r}{R}\right)}{\lambda_n^3 J_1(\lambda_n)} \left(2e^{-\lambda_n^2 \hat{t}} - 1 \right), \quad (24)$$

$$v_{m,r} = v_{\infty} \sum_{n=1}^{\infty} \frac{32}{\lambda_n^4} (2e^{-\lambda_n^2 \hat{t}} - 1), \quad (25)$$

$$\tau_{w,r} = \frac{v_{\infty} \cdot \mu}{R} \sum_{n=1}^{\infty} \frac{16}{\lambda_n^2} (2e^{-\lambda_n^2 \hat{t}} - 1), \quad (26)$$

$$f_r = \frac{64}{Re_{\infty}} \left[4 \sum_{n=1}^{\infty} \frac{(2e^{-\lambda_n^2 \hat{t}} - 1)}{\lambda_n^2} \right] \cdot \left[32 \sum_{n=1}^{\infty} \frac{(2e^{-\lambda_n^2 \hat{t}} - 1)}{\lambda_n^4} \right]^{-2} \quad \text{where} \quad Re_{\infty} = \frac{D \cdot v_{\infty}}{\nu}, \quad (27)$$

In contrast, when the pressure gradient is gradually changed in a linear manner, the final results are even more complicated:

$$v(r, t)_r = v_{\infty} \sum_{n=1}^{\infty} \frac{16 \cdot J_0 \left(\lambda_n \frac{r}{R} \right)}{\lambda_n^3 J_1(\lambda_n)} \cdot F, \quad (28)$$

$$v_{m,r} = v_{\infty} \sum_{n=1}^{\infty} \frac{32}{\lambda_n^4} \cdot F, \quad (29)$$

$$\tau_{w,r} = \frac{v_{\infty} \cdot \mu}{R} \sum_{n=1}^{\infty} \frac{16}{\lambda_n^2} \cdot F, \quad (30)$$

$$f_r = \frac{64}{Re_{\infty}} \left[4 \sum_{n=1}^{\infty} \frac{F}{\lambda_n^2} \right] \cdot \left[32 \sum_{n=1}^{\infty} \frac{F}{\lambda_n^4} \right]^{-2} \quad \text{where} \quad Re_{\infty} = \frac{D \cdot v_{\infty}}{\nu}, \quad (31)$$

where for $0 \leq \hat{t} \leq \hat{t}_r$

$$F = F_1 = 1 - \frac{2}{\lambda_n^2 \hat{t}_r} (\lambda_n^2 \hat{t} + e^{-\lambda_n^2 \hat{t}} - 1), \quad (32)$$

and for $\hat{t} \geq \hat{t}_r$

$$F = F_2 = \frac{1}{\lambda_n^2 \hat{t}_r} (2e^{-\lambda_n^2 (\hat{t} - \hat{t}_r)} - 2e^{-\lambda_n^2 \hat{t}} - \lambda_n^2 \hat{t}_r). \quad (33)$$

3. Verification of the Zielke solution

The analytical solutions discussed in the previous section are distinguished by the assumed pressure gradient driving the flow and appearing on the left in Eq. (1). In the case of flow accelerating from rest, the gradient simply was not there for time $t \leq 0$, and it is positive and constant for time $t > 0$ (Fig. 2a). In decelerated flow, the opposite is assumed, namely a positive value for time $t \leq 0$ and a zero value for $t > 0$ (Fig. 2b). In reverse flow, there is a stepwise (Fig. 2c) or linear (Fig. 2d) change of its sign thereby maintaining the same absolute value (magnitude).

Apart from the discussed analytical solutions, there is a most clever solution which has been derived for any temporal change in the pressure gradient. Its inventor is Zielke. In 1966, in his dissertation [34] and then in an article [35], he used previously known solutions of Eq. (1) by Brown [36] and D'Souza and Oldenburger [37] in the Laplace domain, and he derived its inverse transform (for $g = 0$). From the two-dimensional solution in the Laplace domain he derived a linear (but frequency dependent)

proportionality between the wall shear stress and the average (cross-sectional) velocity. In the time-domain this translates to the following formula relating wall shear stress to average flow acceleration:

$$\tau = \tau_q + \tau_u = \frac{1}{8} \lambda \rho v |v| + \frac{2\mu}{R} \cdot \int_0^t w(t-u) \cdot \frac{\partial v}{\partial t}(u) du. \quad (34)$$

This expression is the sum of the conventional quasi-steady shear stress τ_q and the new time-dependent shear stress τ_u , which is the convolution of a weight function w and the mean acceleration. It is now widely used for calculating non-stationary hydraulic resistance in pipelines during a pressure surge [38-41]. There are two ways of computing the above convolution integral: classic and efficient; in this paper, we will consider the results of both of them.

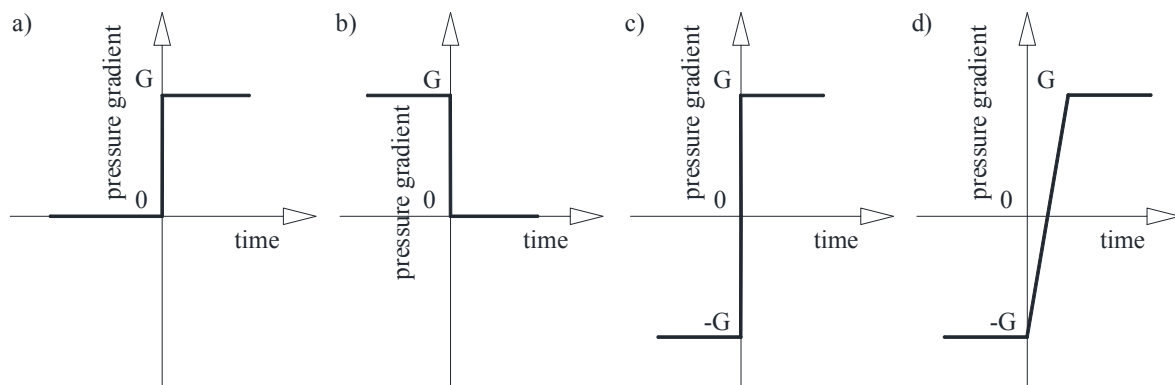


Figure 2. Pressure gradient variation: a) accelerated flow; b) decelerated flow; c) reverse flow (step change); d) reverse flow (linear ramp change).

The classical computation is inefficient, because dealing with all the stored values of changes in flow velocity. The impact of any temporal change of velocity is significant; therefore it is incorporated and weighted by the respective value of the weighting function:

$$\tau_u = \frac{2\mu}{R} \left(\sum_{j=1}^{n-1} \frac{(v_{i,n-j+1} - v_{i,n-j})}{\Delta t} \cdot \int_{(j-1)\Delta t}^{j\Delta t} w(\hat{t}) d\hat{t} \right) = \frac{2\mu}{R} \text{SUM}_c. \quad (35)$$

This form is the classic approach, presented for example by Vardy and Brown [14]. The weight function in the above expression is determined for any dimensionless time from the infinite sum:

$$w_{\text{classic}}(\hat{t}) = \sum_{n=1}^{\infty} e^{-\kappa_n^2 \hat{t}}, \quad (35.1)$$

where: κ_n - n^{th} zero of the Bessel function of type J_2 .

Zielke approximated this function using the following two functions [34,35]:

$$w_{\text{classic}}(\hat{t}) = \sum_{i=1}^6 m_i \hat{t}^{(i-2)/2}, \text{ for } \hat{t} \leq 0.02, \quad (35.2)$$

$$w_{\text{classic}}(\hat{t}) = \sum_{i=1}^6 m_i \hat{t}^{(i-2)/2}, \text{ for } \hat{t} \leq 0.02, \quad (35.3)$$

where: $m_1 = 0.282095$; $m_2 = -1.25$; $m_3 = 1.057855$; $m_4 = 0.9375$; $m_5 = 0.396696$; $m_6 = -0.351563$; $n_1 = 26.3744$; $n_2 = 70.8493$; $n_3 = 135.0198$; $n_4 = 218.9216$; $n_5 = 322.5544$.

Unfortunately, this form is not suitable for use in the efficient solution of the convolution integral:

$$\tau_u(t + \Delta t) = \frac{2\mu}{R} \sum_{i=1}^j \underbrace{[y_{i(t)} A_i + \eta B_i [v_{(t+\Delta t)} - v_{(t)}] + [1 - \eta] C_i [v_{(t)} - v_{(t-\Delta t)}]]}_{y_{i(t+\Delta t)}} = \frac{2\mu}{R} \text{SUM}_e, \quad (36)$$

where:

$$A_i = e^{-n_i \cdot \Delta \hat{t}}; \quad B_i = \frac{m_i}{\Delta \hat{t} \cdot n_i} \cdot [1 - A_i]; \quad C_i = A_i \cdot B_i, \quad (36.1)$$

the idea of which was to reduce the time spent on computation. The number of calculation in this approach depends only on the number of terms describing the effective weight function:

$$w_{\text{effective}}(\hat{t}) = \sum_{i=1}^k m_i e^{-n_i \hat{t}}. \quad (36.2)$$

Formula (36) is a revised Schohl approximation [42]. For the case of water hammer, it was presented and verified in two papers by the first author [15,41]. However, further verification of this new numerical procedure is needed and this will be presented in this section for accelerated, decelerated and reverse laminar flows. The constants A_i , B_i , C_i and η :

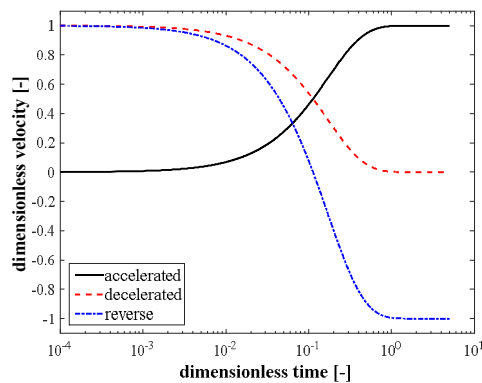
$$\eta = \frac{\int_0^{\Delta \hat{t}} w_{\text{classic}}(\hat{t}) d\hat{t}}{\int_0^{\Delta \hat{t}} w_{\text{effective}}(\hat{t}) d\hat{t}}, \quad (36.3)$$

are determined only once (for the pipe under consideration) at the start of the calculation. The coefficients m_i and n_i found in the formulas (36.1) for the constants A_i , B_i and C_i are suitable constants describing the effective form of the weight function w . Their values are specified in [39]. Additionally, the above procedure is characteristic for the fact that it does not introduce an error for the most recent calculation step. This is most important when using a reduced number of exponential expressions describing the weight function [15]. As seen from formulas (35) and (36), the wall shear stress is a function of temporal changes in the mean velocity and of the weighting function.

3.1. Calculation Example

In order to examine the compatibility of the calculation procedures presented in this section with the analytical solutions given in the previous section, the following examples have been chosen. Accelerated, decelerated and reverse flows of the liquid are considered in a horizontal ($\alpha=0$) pipe with length $L = 250$ m and inner diameter $D = 0.025$ m. The flowing liquid is an oil with density $\rho = 900$ kg/m³ and kinematic viscosity $2.5 \cdot 10^{-5}$ m²/s. The pressure difference $\Delta p = 0.6624$ MPa along the length of the pipe is calculated from the condition that the final (initial in decelerated and reverse flow) Reynolds number is 2300 so that the flow remains laminar. This difference in the case of accelerated flow exists for time $t > 0$, and in the case of decelerated flow for time $t \leq 0$. In reverse flow, a step change of the sign of the above difference is assumed at $t = 0$. Here $G = \Delta p/L = 2.65$ kPa/m (see Fig. 2).

For the above conditions, analytical solutions have been plotted for **accelerated**, **decelerated** and **reverse** flow. They will be designated in detail for $t \geq 0$: **average velocity** from formulas (12), (21) (25) (change of mean velocity over time is illustrated in Fig. 3); **wall shear stress** (13), (22), (26) and the **unsteady coefficient of resistance** (14), (23), (27). The results obtained are compared with the results obtained from convolution-integral methods (35) and (36) discussed briefly in Section 3. Calculations have been performed for a fixed dimensionless time step in the interval from $\Delta \hat{t} = 10^{-4}$ to $\Delta \hat{t} = 5$ (dimensionless time is determined as: $\Delta \hat{t} = v \Delta t / R^2$).

**Figure 3.** Velocity change over time.

The following ratios are of importance:

$$R_{u/q} = \frac{\tau_u}{\tau_q} = \frac{f_u}{f_q} \quad \text{and} \quad R_{\text{tot./q}} = \frac{f}{f_q} = \frac{\tau}{\tau_q}, \quad (37)$$

where: $\tau = \tau_u + \tau_q$ and $f = f_u + f_q$.

The final formulas for the above ratios for the different types of flows are summarised in Table 2.

Table 2. Formulas for the ratios (41).

Ratio	$R_{u/q}$	$R_{\text{tot./q}}$
<i>Roiti-Gromeka-Szymański</i> (accelerated flow)	$\frac{[1-S]}{[1-T]} - 1$	$\frac{[1-S]}{[1-T]}$
<i>Gerbes decelerated flow</i>	$\frac{S}{T} - 1$	$\frac{S}{T}$
<i>Chambré et al. reverse flow</i>	$\frac{X}{Y} - 1$	$\frac{X}{Y}$
<i>Zielke arbitrary flow</i>	$\frac{\text{SUM}}{2v_{(t+\Delta t)}}$	$\frac{\text{SUM}}{2v_{(t+\Delta t)}} + 1$

where: $S = 4 \sum_{n=1}^{\infty} \frac{e^{-\lambda_n^2 \hat{t}}}{\lambda_n^2}$; $T = 32 \sum_{n=1}^{\infty} \frac{e^{-\lambda_n^2 \hat{t}}}{\lambda_n^4}$; $X = 4 \sum_{n=1}^{\infty} \frac{2e^{-\lambda_n^2 \hat{t}} - 1}{\lambda_n^2}$; $Y = 32 \sum_{n=1}^{\infty} \frac{2e^{-\lambda_n^2 \hat{t}} - 1}{\lambda_n^4}$

SUM = SUM_c (in classic solution – (35)); SUM = SUM_e (in efficient solution – (36))

The results obtained, showing the change in total shear stress over time, for the three analysed flows, are shown in the Figs 4a-4c. They indicate correctly that the values in the case of accelerated flow (Fig. 4a) increase from zero to a constant value equal τ_q , and that in decelerated flow (Fig. 4b) they decrease from the value τ_q to zero. The rapid decrease of the slope of the curve in Fig. 4a in the vicinity of the dimensionless time $\hat{t} = 1$ can be linked to the formation of a parabolic flow profile. Thus, the parabolic profile is formed only in the last phase of the acceleration. A different situation is observed in Fig. 4b, where there is a very slow relative change in shear stress, thus it can be assumed that the parabolic flow profile remains for quite a long time until the final stopping phase around time $\hat{t} = 0.22$. After that time curve have a rapid increase and flow profile cannot be assumed as parabolic anymore. In the example involving reverse flow (Fig. 4c), it can be seen that the stress correctly changes from a positive to a negative quasi-steady value. Complete reversal of flow, seen as a deceleration followed by an acceleration, is complete after $\hat{t} = 2$.

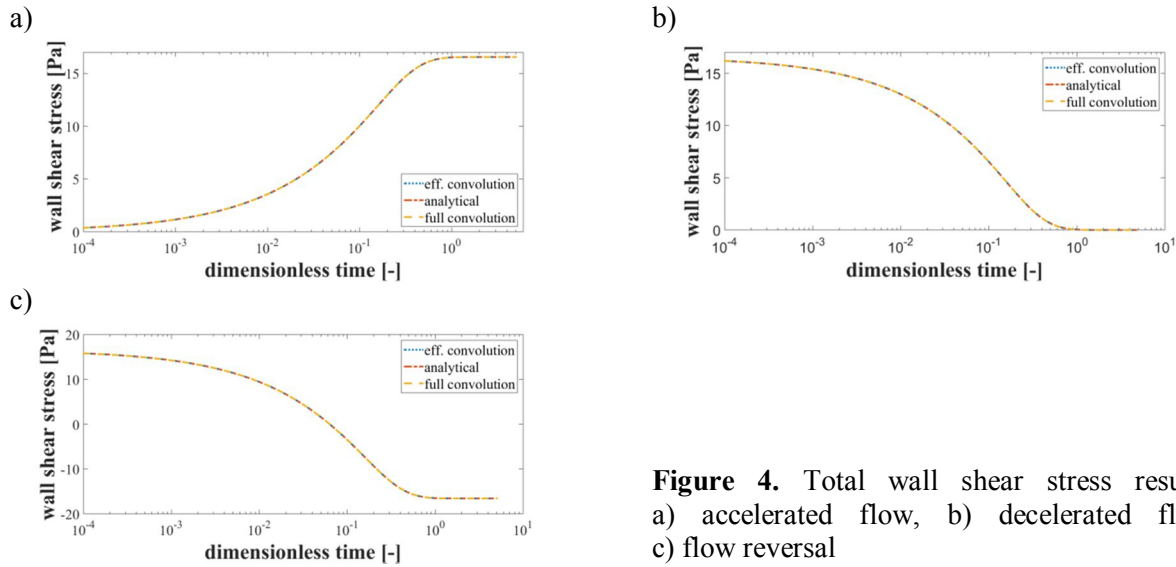


Figure 4. Total wall shear stress results: a) accelerated flow, b) decelerated flow, c) flow reversal

The results obtained for the change of the ratio $R_{u/q}$ of time dependent wall shear stress τ_u to quasi-steady wall shear stress τ_q and/or time dependent friction factor f_u to quasi-steady one f_q over time, for the three analysed flows, are shown in the Figs 5a-5c.

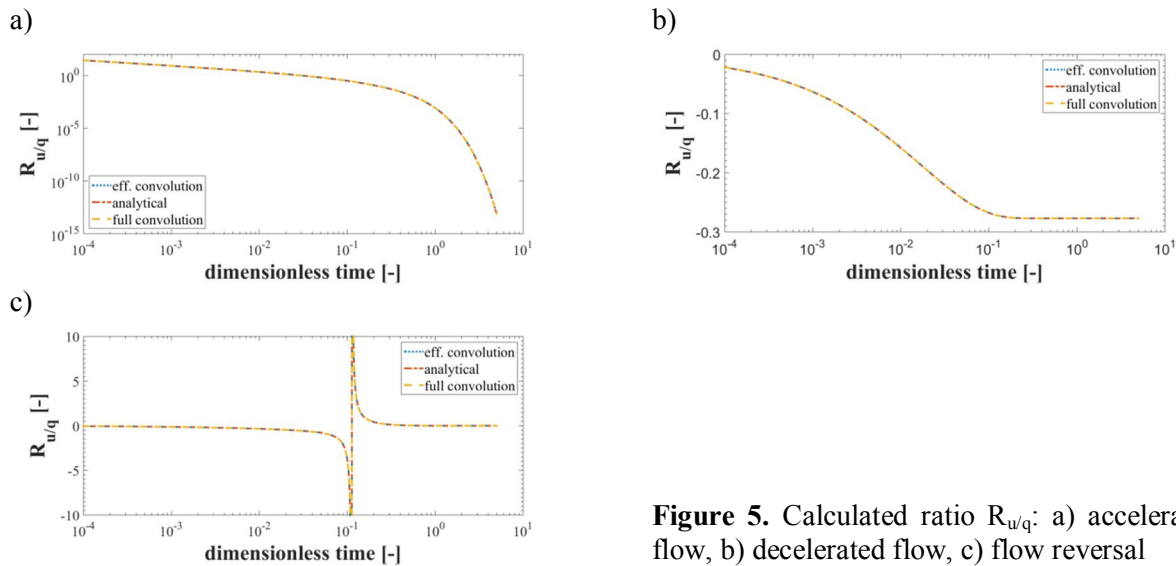


Figure 5. Calculated ratio $R_{u/q}$: a) accelerated flow, b) decelerated flow, c) flow reversal

The results of the $R_{u/q}$ ratio show that the initial phase of accelerated flow (Fig. 5a) is dominated by unsteady wall stress ($\tau_u > \tau_q$ for $\hat{t} < 0.03$). This situation is reversed for times $\hat{t} > 0.03$ (since henceforth $\tau_u < \tau_q$). In decelerated flow (Fig. 5b), the τ_u calculated is negative ($\tau_u < 0$), since along with the duration of this flow, the subsequent average flow velocity values decrease, and the quasi-steady component τ_q remains positive until the end. From time $\hat{t} > 0.45$, this ratio stabilises to the value -0.28 , which is the final results for large dimensionless times (taking into account first terms of sums in S/T-1 one get $(4/32) \cdot \lambda_1^2 - 1 \approx -0.28$). This means that the unsteady wall stress τ_u affects significantly the total shear stress τ until the complete stop of fluid flow. Analysing the results for reverse flow (Fig. 5c), it can be seen that decelerating occurs in the initial phase. Just before $\hat{t} = 0.11$, the values of $R_{u/q}$ approach $-\infty$ because τ_q vanishes. However, after exceeding this reversal time and corresponding singularity, there is an acceleration of the liquid and $R_{u/q}$ ratio returns from $+\infty$ to reach the value of approximately 1 when $\hat{t} = 2$.

Figures 6a-6c show the ratio $R_{\text{tot./q}}$ of the total friction factor f to the quasi-steady one f_q and/or total wall shear stress τ to the quasi steady one τ_q , for the three analysed unsteady flows. In the case of accelerated flow (Fig. 6a), we can see that the resulting value moves from ∞ to 1 (steady flow). This means that the time dependent friction factor f_u in accelerated flow is greater than in quasi-steady flow f_q . The next graph (Fig. 6b) shows that in decelerated flows, the total friction factor f adopts values smaller than that calculated using the quasi-steady formula. But what is important time dependent friction factor f_u plays an important role until the final stop of flow as evidenced by the value $R_{\text{tot./q}} = 0.723$ which this ratio tends to with increasing dimensionless time. In reverse flows (Fig. 6c), this ratio before changing the direction of flow reaches negative values (from $\hat{t} > 0.06$) and later approaches $-\infty$.

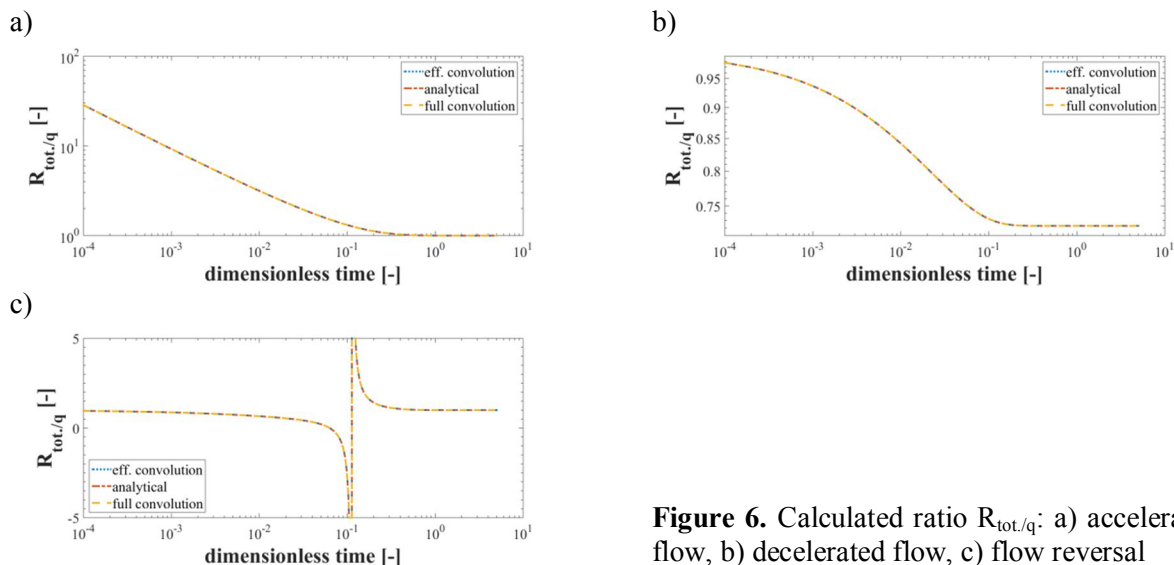


Figure 6. Calculated ratio $R_{\text{tot./q}}$: a) accelerated flow, b) decelerated flow, c) flow reversal

The appearance of negative values is related to the fact that the liquid flow direction changes more rapidly near to the pipe wall (Fig. 7). A zero value of the average velocity occurred in the analysed flow for time $\hat{t} = 0.11$. Just after this time, this ratio reaches the value of $+\infty$, before falling to a value of unity (no effect of unsteady flow).

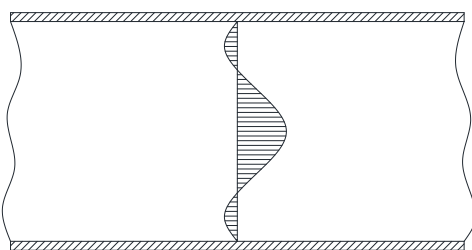


Figure 7. Back flow near the wall

4. Summary

The results presented in this paper clearly show that both the improved Zielke solution (35) and the more efficient solution of the convolution integral (36) describe very well the unsteady laminar flow resulting from acceleration, deceleration, or reversal of liquid in a pipe. The graphs show no significant differences between the analytical and numerical results. Subtle differences between the efficient and the classical solution of the convolution integral are not shown herein but were noted in an extensive analysis of relative errors carried out during the preparation of this paper.

Historical references [1-3] collected and analysed for the purpose of this paper allow the statement that the solution known in the literature relating to accelerated laminar pipe flows, the authorship of which was originally transcribed to Szymański in 1932, had been derived already sixty years earlier in 1871

by Roiti and later on in 1882 by Gromeka. Therefore, referring to these solutions, we should include the names of all authors who have derived them apparently independently: Roiti-Gromeka-Szymański.

While working on these solutions, we can see a heat-conduction analogy. Since the issues of heat conduction have been dealt with since the beginning of the nineteenth century, one can suppose that the same final formulas could have been derived by someone even earlier than 1871 for some special case of non-stationary heat flow - perhaps in a hollow cylinder.

The universal solutions presented in Section 2.3 may be used in any inclined straight pipe with accelerated flow in any direction.

References

- [1] Roiti A 1871 Sul movimento dei liquidi *Annali della Scuola Normale Superiore di Pisa – Classe di Scienze* **1** (in Italian) 193
- [2] Gromeka I S 1882 On a theory of the motion of fluids in narrow cylindrical tubes *Uch. Zap. Kazan. Inst.* **112** (41) (in Russian)
- [3] Szymański P 1932 Quelques solutions exactes des équations de l'hydrodynamique du fluide visqueux dans le cas d'un tube cylindrique *J. Math. Pures et Appliquées* **11(9)** (in French) 67
- [4] Gerbes W 1951 Zur instationären, laminaren Strömung einer inkompressiblen, zähen Flüssigkeit in kreiszylindrischen Rohren *Zeitschrift für angewandte Physik* **3(7)** (in German) 267
- [5] Poisson S D 1823 Mémoire sur la distribution de la chaleur dans les corps solides *Journal de l'Ecole Polytechnique* **12** (in French) 1
- [6] Poisson S D 1831 Mémoire sur les équations générales de l'équilibre et du mouvement des corps solides élastiques et des fluides *Journal de l'Ecole Polytechnique* **13** (in French) 1
- [7] Poisson S D 1835 Théorie Mathématique de la Chaleur, Paris: Bachelier (in French)
- [8] Betti E 1868 Alcune determinazioni delle temperature variabili di un cilindro, Pisa, *Tip. Nistri* (in Italian)
- [9] Betti E 1868 Sopra la determinazione delle temperature nei corpi solidi ed omogenei, Firenze, *Stamperia Reale* (in Italian)
- [10] Fassò C A 1956 Avviamento del moto di una corrente liquida in un tubo di sezione costante: Influenza delle resistenze *Reniconti Istituto Lombardo – Accademia di Scienze e Lettere* **90** (in Italian) 305
- [11] Ghidaoui M S and A A Kolyshkin 2002 A Quasi-steady approach to the instability of time dependent flows in pipes *Journal of Fluid Mechanics* **465** 301
- [12] Szymański P 1930 Sur l'écoulement non permanent du fluide visqueux dans le tuyau *Compte Rendu du III Congrès International de Mécanique Appliquée Stockholm* (in French) 249
- [13] Chambré P L et al. 1978 Reversal of laminar flow in a circular pipe *Nuclear Engineering Design* **47** 239
- [14] Vardy A E and Brown J M B 2010 Evaluation of unsteady wall shear stress by Zielke's method *J. Hydraul. Eng.* **136** 453
- [15] Urbanowicz K 2015 Simple modelling of unsteady friction factor *Proc. BHR Group - 12th International Conference on Pressure Surges Dublin* 113
- [16] Reynolds O 1883 An experimental investigation of the circumstances which determine whether the motion of water shall be direct or sinuous, and of the law of resistance in parallel channels *Philosophical Transactions of the Royal Society of London* **174** 935
- [17] Iguchi M et al 2010 Effect of initial constant acceleration on the transition to turbulence in transient circular pipe flow *Journal of Fluids Engineering* **132**
- [18] Vardy A E and Brown J M B 2011 Laminar pipe flow with time-dependent viscosity *Journal of Hydroinformatics* **13** (4) 729
- [19] Muzychka Y S and Yovanovich M M 2006 Compact models for transient conduction or viscous transport in non-circular geometries with a uniform source *International Journal of Thermal Sciences* **45** 1091

- [20] Muzychka Y S and Yovanovich M M 2010 Unsteady viscous flows and Stokes's first problem *International Journal of Thermal Sciences* **49** 820
- [21] Telionis D 2012 Unsteady viscous flows *Springer Series in Computational Physics*
- [22] Lam F 2015 On exact solutions of the Navier-Stokes equations for uni-directional flows *arXiv:1503.05149v3 [physics.flu-dyn]*
- [23] Chaudhury R A et al. 2015 Length and time for development of laminar flow in tubes following a step increase of volume flux *Exp Fluids* **56** (22)
- [24] Pontrelli G 2000 Blood flow through a circular pipe with an impulsive pressure gradient *Mathematical Models and Methods in Applied Sciences* **10** (2) 187
- [25] Drazin P G and Riley N 2006 The Navier-Stokes equations: A classification of flows and exact solutions *London Mathematical Society Lecture Note Series* **334** Cambridge University Press
- [26] Constantinescu V N 2012 Laminar viscous flow (Mechanical Engineering Series) *Springer*
- [27] Urbanowicz K and Tijsseling A S 2015 Work and life of Piotr Szymański *Proc. BHR Group - 12th International Conference on Pressure Surges* Dublin 311
- [28] Loitsyanskii L G 1966 Mechanics of Liquids and Gases (first English edition) *Oxford: Pergamon Press*
- [29] Martin C S and Wiggert D C 2013 Discussion of "Evaluation of unsteady wall shear stress by Zielke's method" by Alan E. Vardy and Jim M. B. Brown. *ASCE Journal of Hydraulic Engineering* **139** 562
- [30] Gromeka I S 1952 Collected Works, *USSR Academy of Sciences*, Moscow (in Russian) 149
- [31] <http://books.e-heritage.ru/book/10079943>
- [32] Çengel Y A and Cimbala J M 2006 Fluid Mechanics: Fundamentals and Applications. *Boston: McGraw-Hill Higher Education*
- [33] Urbanowicz K 2012 New approximation of unsteady friction weighting functions *Proc. of the 11th International Conference on Pressure Surges* Lisbon 477
- [34] Zielke W 1966 Frequency-dependent friction in transient pipe flow *University of Michigan* (Phd thesis)
- [35] Zielke W 1968 Frequency-dependent friction in transient pipe flow *Trans. ASME, J. Basic Engng* **90** 109
- [36] Brown F T 1962 A The transient response of fluid lines *Trans. ASME, J. Basic Engng* **84** 547
- [37] D'Souza A F and Oldenburger R 1964 Dynamic response of fluid lines *Trans. ASME, J. Basic Engng* **86** (3) pp. 589-598
- [38] Zarzycki Z et al. 2011 Improved method for simulating transients of turbulent pipe flow *Journal of Theoretical and Applied Mechanics* **49** (1) 135
- [39] Urbanowicz K and Zarzycki Z 2012 New efficient approximation of weighting functions for simulations of unsteady friction losses in liquid pipe flow *Journal of Theoretical and Applied Mechanics* **50** (2) 487
- [40] Urbanowicz K et al. 2012 Universal weighting function in modeling transient cavitating pipe flow *Journal of Theoretical and Applied Mechanics* **50** (4) 889
- [41] Urbanowicz K and Zarzycki Z 2015 Improved lumping friction model for liquid pipe flow *Journal of Theoretical and Applied Mechanics* **53** (2) 295
- [42] Schohl G A 1993 Improved approximate method for simulating frequency-dependent friction in transient laminar flow *Trans. ASME, Journ. of Fluids Eng.* **115** 420